Archives of Materials Science and Engineering

Volume 56
Issue 1
July 2012
Pages 5-21

International Scientific Journal
published monthly by the
World Academy of Materials
and Manufacturing Engineering

Fabrication methods and heat treatment conditions effect on structure and properties of the gradient tool materials

L.A. Dobrzański, A. Kloc-Ptaszna*, M. Pawlyta, W. Pakieła

Institute of Engineering Materials and Biomaterials, Silesian University of Technology,
ul. Konarskiego 18a, 44-100 Gliwice, Poland
* Corresponding e-mail address: anna.kloc-ptaszna@polsl.pl

Received 07.05.2012; published in revised form 01.07.2012

ABSTRACT

Purpose: This work concerns manufacturing and research on a new group of the gradient tool materials, manufactured by the conventional powder metallurgy method, consisting in compacting a powder in a closed die and sintering it.

Design/methodology/approach: The materials were obtained by mixing the powders of the HS6-5-2 high-speed steel, tungsten carbide (WC). The mixes were poured one after another into the die, yielding layers with the gradually changing volume ratio of carbides within the high-speed steel matrix. Structural research by using the scanning and transmission electron microscopes, x-ray microanalysis and density, hardness and porosity tests, were performed. Structure and hardness of selected materials after heat treatment were also investigated. The pin on plate test was used in order to examine the tribological properties of the analyzed materials.

Findings: On the basis of the results of the research, it was found that it is possible to obtain gradient materials by the powder metallurgy methods, in order to ensure the required properties and structure of the designed material. It was shown that the new sintered graded materials are characterized by a multiphase structure, consisting of ferrite, primary carbides of the high speed steel, of the MC and M6C type, and dependently of the reinforcement phase, of the tungsten carbide WC which are introduced into the material, in the powder form. It has been proved by the pin on plate test that the addition of the tungsten carbide to the high-speed steel significantly improved the tribological properties.

Practical implications: Developed material is tested for turning tools.

Originality/value: The material presented in this paper has layers consisting of the carbide-steel with growing hardness on one side, and on the other side the high-speed steel, characterized by a high ductility.

Keywords: Gradient tool materials; Uniaxial pressing; Sintering; High-speed steel; Tungsten carbide

Reference to this paper should be given in the following way:

L.A. Dobrzański, A. Kloc-Ptaszna, M. Pawlyta, W. Pakieła, Fabrication methods and heat treatment conditions effect on structure and properties of the gradient tool materials, Archives of Materials Science and Engineering 56/1 (2012) 5-21.

MATERIALS

1. Introduction

Several main gradient materials fabrication methods were developed to date, like: powder metallurgy methods, coating deposition methods, and methods based on diffusion phenomenon [1-10]. Material's gradient structure may be obtained, among others, by strengthening the matrix with precipitations or particles with various properties, sizes, and shapes, with the portions changing in the material volume [1-3]. Powder metallurgy is the method making it possible to implement relatively easily the distribution control of the reinforcing phases particles in the matrix, ensuring full use of the feedstock, and very high repeatability of the results obtained. This method makes it possible to combine various components to obtain the required material properties that cannot be obtained economically with other methods. Many research projects pertaining to the sintered materials indicate that materials with the precisely specified chemical composition and high purity can be obtained thanks to powder metallurgy method [11-32]. Fabrication of sintered materials is divided into three main stages, i.e., fabrication of powders, forming of powders, and sintering [33]. There are many powder forming methods, like die uniaxial compacting, cold isostatic pressing of the polymer-powder slurry, vibratory forming and additional compaction in the closed die, and the sedimentation forming. As it turns out from the literature review, forming by filling and compacting powders in the die is the most common powder forming method in the laboratory conditions [33-36]. This method is easier from the technological point of view in realization compared to other forming methods. Moreover, this method can be easily applied in the industrial conditions using the conventional presses. Materials with the smooth structure porosity may be obtained by pouring the mixture of powders with the diverse shape of their particles or by a change of compaction conditions. However, obtaining materials with the changing pores size may be obtained by varying the powder particles sizes. One can also obtain the material structure characteristic of the smooth change of the chemical- and phase compositions using the powder metallurgy method, by pouring mixtures with the various portions of the matrix material powders with the powders of material that would have to perform the strengthening function [37-38]. If the differences of portions of the relevant phases in the particular layers are small, due to phenomena occurring during sintering (among others diffusion) there are no clear boundaries between the particular layers and the structure of the obtained material is characteristic of smooth changes of portions of the particular phases. Research pertaining the sintered tool gradient materials are ongoing in various research centers domestic and abroad. The results obtained indicate that thanks to the powder metallurgy method it is possible to fabricate materials characteristic of structure varying in the material's volume along with its chemical- or phase composition change. Therefore, the metal powder metallurgy method consisting in the uniaxial compacting of the powder in the closed die, with its subsequent sintering, seems to be advantageous for fabrication of the new gradient tool materials.

Material with the relatively high core ductility and high surface hardness, and consequently high abrasion wear resistance, is the tool material sought. Therefore, the gradient tool materials should be designed to ensure the high abrasion wear resistance in the working layer, retaining the ductile core, making withstanding the high dynamic loads possible. Literature review pertaining to tool materials suggests that the highest plasticity is characteristic of the high-speed steel from among all tool materials mentioned above. Importance of the high-speed steels remains still high in spite of the intensive development of other groups of tool materials. Moreover, development of the manufacturing technology - employment of powder metallurgy methods - has added to improvement of the service properties of the discussed steels. Thanks to the fine-grained structure characteristic of the uniform distribution of the primary carbides, and lack of carbides separation and banding, as for the conventional high-speed steel, the ductility of the steel sintered after hardening and tempering is higher than ductility of a steel fabricated with the conventional method. Therefore, the sintered high-speed steels feature the dominating group of tool materials used when the especially desired property of the sintered tool material is its relatively high ductility [39-43].

The second desirable property of the tool material sought is its high hardness, which should exceed hardness of the machined material by at least 30 HRC [41]. Sintered carbides, among the tool materials, are characteristic of the relatively high hardness (1900-2500 HV). However, the significant brittleness of these materials limits their applications range because of the dynamic external loads occurring in service of the cutting tools [44].

High-speed steel matrix composites are characteristic of properties intermediate between the high-speed steels and sintered carbides. These materials are included into the group of sintered composites with metal matrix reinforced with particles. An advantage of the cermets is the fact that their mechanical properties can vary in a broad range depending on the matrix type and heat treatment state [36,41,44]. Research ongoing currently in various scientific centers are focused on fabrication of composites based on the high-speed steels with the improved abrasion wear resistance. Addition effect of WC, TiC, VC, and NbC carbides on structure and properties of the HSS matrix based composites was investigated in works [3, 45-47]. It was found out that along with the relative volume increase of carbides in the high-speed steel matrix composites their hardness and abrasion wear resistance grow; however, their bending strength decreases. One should also take into account that the secondary hardness effect occurring during tempering of the high-speed steels, connected with precipitation of the dispersive carbides in the martensitic matrix and transformation of the retained austenite during high-temperature tempering, which may feature an additional precipitation hardening mechanism of the gradient materials, apart from the dispersive hardening by the increased portion of the reinforcing phases particles.

Keeping in mind all factors mentioned above, beginning of research was assumed to be purposeful pertaining to development of the new group of the high-speed steel matrix composites, reinforced with the hard WC carbide phases, development of their fabrication technology as well as determining their structure and properties.

2. Material for investigation

Powders of the HS6-5-2 high-speed steel and tungsten carbide (WC) were used for fabrication of the gradient tool materials. The particles of the HS6-5-2 high-speed steel powders particles are shown in Figure 1 and WC powders particles are shown in Figure 2. Chemical compositions and main properties of these powders are presented in Table 1.

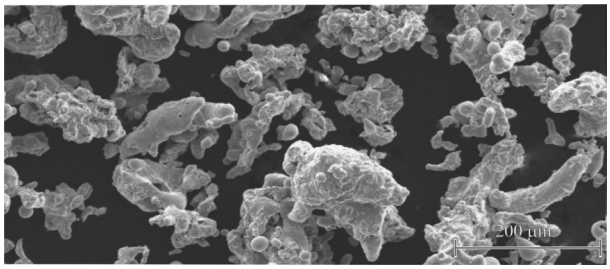

Fig. 1. Scanning electron micrographs of HS6-5-2 powders

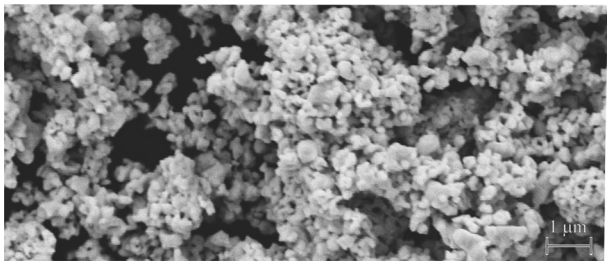

Fig. 2. Scanning electron micrographs of WC powders

Table 1.
Properties and chemical composition of powders

	Mass concentration, %	
Element	HS6-5-2	WC
C	0.75-0.90	6.11
Mn	0.20-0,45	-
Si	≤ 0.45	≤ 0.002
P	≤ 0.04	-
S	≤ 0.04	0.003
Cr	3.75-4.5	-
Ni	0.2	-
Mo	4.5-5.5	≤ 0.001
W	5.50-6.75	rest
V	1.6-2.2	0.19
Co	0.1	-
Cu	0.1	-
Fe	rest	0.003
Ca	-	0.003
Al	-	≤ 0.002
Mg	-	≤ 0,001
K	-	≤ 0.001
Na	-	≤ 0.001
C free	-	0.02
Grain size, µm	> 150	> 0.86
Additional information	High-speed steel powder, atomised with water, made by HOEGANAES	Tungsten carbide powder made by Baildonit

3. Investigation methodology

The investigation was carried out in three stages. The optimum concentration was selected at the first stage for the particular constituents of the surface layer of the designed materials, using the same sintering parameters (sintering temperature, T_s=1250°C; sintering time, t_s=60 min) [48].

The second stage concerned fabrication of the tool gradient high-speed steel matrix composites with the surface layers selected experimentally at the first stage. Two types of green compacts were fabricated with four layers. Surface layers contain 90HSS/10WC, 75HSS/25WC. The consecutive intermediate layers were constituted from the surface layer side, with the decreasing concentration of the WC tungsten carbides, down to the substrate layer containing the high-speed steel only. It was assumed that such composition of layers may correspond to the material intended for fabrication of the turning tools.

Powder mixes were poured one after the other into the die yielding layers with the gradually changing percentage volume portions of carbides in the high-speed steel. For concentration in the surface layer of 25% WC the next intermediate layers were constituted containing 15% and 5% of these carbides respectively. In case of the surface layer with the 90HSS/10WC composition, the intermediate layers contain 7% and 4% WC respectively.

The test pieces were compacted under the pressure of 500 MPa. Selection of the sintering parameters was made experimentally by variation of the green compacts' sintering temperature, time, and atmosphere. The test pieces were sintered in the vacuum furnace and in the furnace with the flowing atmosphere of nitrogen with addition of N_2 + 5% H_2, at the temperatures of 1210, 1230, 1250, and 1270°C, for 30 and 60 minutes.

Based on structure observations and examinations as well as on test results of density, hardness, and porosity, optimum concentrations were selected of the constituents in the particular material layers. Based on analyses carried out the gradient material was selected for further investigations with the high-speed steel reinforced with the WC tungsten carbide with the 75HSS/25WC surface layer composition (Fig. 3).

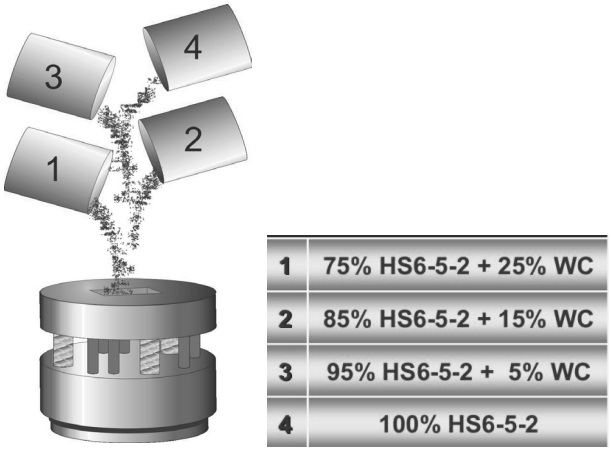

Fig. 3. The proportions of the constituents of the compacted and sintered four-layer test pieces

At the third stage the batch of test pieces was made for heat treatment and for testing of mechanical properties and examination of the gradient material in the quenched and tempered states. At the third stage a set of test pieces was prepared to carry out their heat treatment. The powders were mixed for an hour. Four consecutive layers were poured into the die, with the relevant compositions from the 75HSS/25WC surface layer, through the 85HSS/15WC, 95HSS/5WC intermediate layers, up to the high-speed steel alone. The compaction was carried out under the pressure of 500 MPa. Sintering was carried out at the temperature of 1210°C for 30 minutes. The rate of heating up and cooling down to the sintering temperature was selected experimentally and it is equal to 5°C/min. The sintered test pieces were subjected to heat treatment. The heat treatment conditions are presented in Table 2.

Table 2.
The heat treatment conditions

T_a – austenitizing temperature, °C	t_a – austenitizing time, s	$T_{tI,II}$ – tempering temperature I and II, °C
1120	80	470
1150	120	500
1180	160	530
1210		560
		590

4. Own research

4.1. Structure examinations

Metallographic examinations were made on microsections of the sintered and heat treated test pieces. Test pieces were cut in the plane perpendicular to the outer layer on the 'Isomet-4000' (BUEHLER) cut-off machine using water jet cooling. Next they were hot-mounted in the thermosetting resin, ground using the abrasive papers with the 180-2400 μm/mm^2 grain size at 300 rpm, and buffed on diamond compounds at 150 rpm.

Microsections of the sintered test pieces were etched in nital (3% solution of nitric acid in ethanol) making observations possible of the light, non-etching carbides on the dark etched matrix; whereas, microsections of the hardened test pieces were etched in the etchant containing 5 g picric acid, 100 ml purified water, 0.5 g sodium alkylsulfonate, to reveal the primary austenite grains boundaries.

Metallographic examinations were made on the light microscopes (Leica MEF4A and OPTON Axiovert) at magnifications from 100 to 1000 x, and on the scanning electron microscopes (Philips XL30 and Zeiss Supra 35) equipped with the secondary electron detectors (SE) and back scattered electron detectors (BSE or QBSD) at the accelerating voltage from 5 to 20 kV, at magnifications from 50 to 10000 x.

The primary austenite grain size was measured with Snyder-Graff method.

Volume portions of carbides were determined with the quantitative metallography methods using the Image-Pro Plus computer image analysis computer system.

Assessment of phase compositions of powders, compacts, and gradient high-speed steel matrix composites in the sintered - and heat treated states was carried out using the PANalytical X'PertPRO X-ray diffractometer using the filtered K radiation of the cobalt lamp at 40 kV voltage and 30 mA heater current. The reflected radiation intensity measurements were made in the 2θ angle range from 30 to 120° every 0.05° and counting time of 10 seconds.

The retained austenite volume portion was calculated using software developed in the Department of Materials Processing Technology, Management, and Computer Techniques in Materials Science. The software makes it possible to calculate the volume portion of the retained austenite in steels with the Averbach-Cohen roentgenographic method based on measurement results of the complete intensities of diffraction maxima of the X-ray radiation from the γ and α phases lattice planes. It was assumed in calculations that the X-ray radiation intensity deflected on the crystallographic planes of γ and α phases is proportional to the portions of these phases in steel.

4.2. Examination of physical and mechanical properties

Measurement of density, porosity and hardness with testing with Vickers and Rockwell in A scale methods were made on the sintered test pieces.

Densimetric method was used to measure the density of sintered test pieces, consisting in measurement of the apparent test piece mass when immersed in water.

Hardness testing with Vickers method was made at the indenter load of 4.903 N. Duration of the total indenter load was 15 s. The test was carried out on the entire transverse section width of the sintered test pieces, beginning from the distance of 0.2 mm from the external face of the surface layer up to the substrate layer zone (about four test points fell to each layer). Hardness tests with Rockwell in scale A were made on the end faces of the surface layers of the sintered gradient high-speed steel matrix composites. Tests were made at 10 locations selected randomly from the surface layers zones.

Hardness tests with Rockwell in scale C were made on the end faces of the surface layers of the heat treated gradient high-speed steel matrix composites. For each heat treatment variant tests were made at randomly selected locations from the surface layers and substrate zones (10 measurements for each layer). Hardness tests were also made of the test pieces from the selected MG-75HSS/25WC material in the sintered state to compare the HRC hardness test results of materials before and after heat treatment.

Test results for density, porosity and hardness were analysed statistically, by calculating the arithmetic average, standard deviation, and confidence interval for each test series at the significance level $\alpha = 0.05$. The linear correlation coefficient was calculated for hardness and density measurement results of the sintered gradient high-speed steel matrix composites, and its test of significance was made.

To measure the resistance to abrasion the tribometer SCM INSTRUMENTS was used. The abrasion resistance was measured by using the tribometer SCM INSTRUMENTS. The material was tested at a load of 10 N, speed of 7.54 cm/s and two different cycle numbers (10000 and 20000). The tests were performed at the measuring distance equal to 4mm. The measuring length was equal 0.8 mm and gauge range from 0 to 10um (which ensured high precision of measurements) was applied for the wear profile. The ceramic ball (Al_2O_3) was used as the counter sample with 6mm radius. The hardness of the counter samples was higher than the hardness of the sample. The profile of wear was measured using the profilometer SURTRONIC 25 TAYLOR HOBSON. Pin on plate test was carried along the cross-sections along the sample. Such measurements showed all the layers of the sample from the ground to a surface with the highest concentration of carbides.

5. Test results of the gradient sintered high-speed steel matrix composites

5.1. Density, porosity and hardness

The density measurement results obtained for the high-speed steel matrix composites reinforced with the WC tungsten carbide, sintered in the vacuum furnace and in the furnace with the atmosphere of the flowing nitrogen with the addition of hydrogen (N_2 + 5%H_2) are presented in Figures 4-9.

The highest density in case of the gradient cermets with the surface layer with the 90M2/10WC composition is ca. 8.22 g/cm^3). Extension of the sintering time to 60 minutes results also in a slight density growth (Figures 4-9). The maximum average density of ca. 8.49 g/cm^3 occurs in the test piece with the surface layer containing 75HSS/25WC after sintering at the temperature of 1230°C. Density of the test piece with 10% tungsten carbide portion in its surface layer changes from ca. 6.42 g/cm^3 at the temperature of 1210°C to the maximum one of ca. 8.09 g/cm^3 at the sintering temperature of 1270°C. Extension of the sintering time to 60 minutes does not result in a significant density growth.

The HRA hardness test results obtained for the face surfaces of the gradient high-speed steel matrix composites sintered in the vacuum furnace and in the furnace with the atmosphere of the flowing nitrogen with the addition of hydrogen (N_2+5%H_2) are presented in Figures 10-15.

The test piece with the surface layer of the 90HSS/10WC composition has the lowest average hardness at the temperature of 1210°C - ca. 68.54 HRA. The average hardness grows with the sintering temperature increase to the value of ca. 80.5 HRA for the test piece sintered at the temperature of 1270°C. Increase of WC concentration in the gradient material also results in hardness growth.

The average hardness for test pieces with the surface layer containing 25% WC, after sintering at the temperature of 1230°C, is ca. 81.2 HRA for T_s=1210°C and ca. 83.5 HRA. Extension of the sintering time to 60 minutes, in the same sintering conditions, in the temperature range from 1210 to 1270°C does not cause big hardness changes of the investigated gradient high-speed steel matrix composites compared to hardness after sintering for 30 minutes. The maximum hardness of ca. 83.1 HRA occurs in the test piece with the surface layer containing 75HSS/25WC after sintering at the temperature of 1230°C.

The minimum average hardness (ca. 56.7 HRA) was obtained for the test pieces sintered the temperature of 1210°C; whereas, the maximum one (ca. 80.6 HRA) for the test pieces sintered the temperature of 1270°C. After sintering in the same conditions hardness of the surface layer with a higher content of the WC tungsten carbide (25%) exceeds hardness of the 90HSS/10WC one. The maximum average hardness for this test piece is ca. 84.2 HRA after sintering at the temperature of 1230°C.

The sintering temperature increase affects substantially hardness of the test pieces containing 90HSS/10WC. The average hardness of the surface layer nearly doubles from ca. 43.2 HRA for the test piece sintered at the temperature of 1210°C to ca. 80.1 HRA for the test piece sintered at the temperature of 1270°C. The maximum hardness of ca. 84.2 HRA was obtained in the test pieces with the surface layer containing 75HSS/25WC for the test piece sintered at the temperature of 1230°C.

Figures 16 to 17 illustrate the regression function plots describing the relationship between HV hardness and the measuring point location, sintering temperature and sintering time for materials in a vacuum furnace and Figs. 18 and 19 for the furnace with the atmosphere of flowing nitrogen with addition of hydrogen (N_2+5% H_2). The results of HV hardness measurements show a gradient variation in the properties of the tested materials in their volume. The hardness value of all the tested materials, regardless the sintering conditions, changes along with the changing distance of the measuring point from the outer surface of the surface layer. The hardness of GM-90HSS/10WC sintered in vacuum depending on the sintering temperature is within 500-800 HV in the surface layer and decreases along with the growing distance between the measuring point and the outer surface of the surface layer up to 270-510 HV in the substrate layer. The hardness of GM-90HSS/10WC sintered in the atmosphere of the flowing gas mixture (N_2+5% H_2) is within 580-680 HV in the surface layer and also declines along with the growing distance of the measuring point from the outer surface of the surface layer up to 350-540 HV. In GM-75HSS/25WC where the fraction of the WC reinforcing fraction in the individual layers is higher (25% of WC in the surface layer), a hardness variation increases by approx. 100 HV in the surface layer. For GM-75HSS/25WC sintered in vacuum, it is within the range of 600-900 HV and decreases to 250-470 HV, and for GM-75HSS/25WC sintered with the atmosphere of the flowing mixture of gases, it is 300-860 HV in the surface layer and decreases along with the growing distance of the measuring point from the outer surface of the surface layer to 240-510 HV in the substrate layer.

The regression function plot describing the relationship between porosity and the fraction volume of the reinforcing phase in the individual layers and sintering temperature is shown in Fig. 20. It was found that the area with higher porosity in the materials sintered at 1210°C is limited only to the surface layers and disappears almost completely along with the growing sintering temperature.

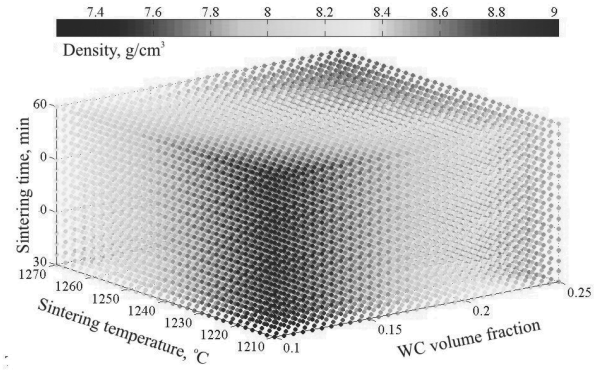

Fig. 4. Regression function plot describing relationship between density and the volume fraction of the reinforcing phase, temperature, and sintering time, for the gradient material reinforced with WC carbide, sintered in the vacuum furnace

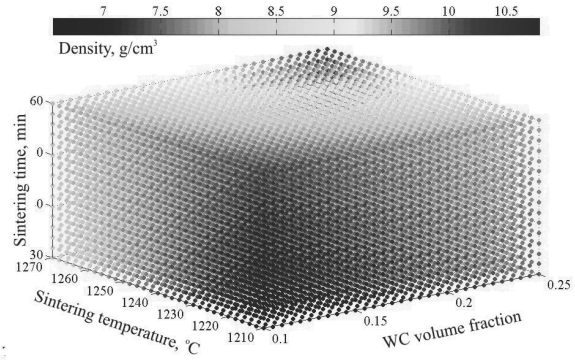

Fig. 7. Regression function plot describing relationship between density and the volume fraction of the reinforcing phase, temperature, and sintering time, for the gradient material reinforced with WC carbide, sintered in furnace with the atmosphere of the flowing nitrogen with addition of hydrogen (N_2+5%H_2)

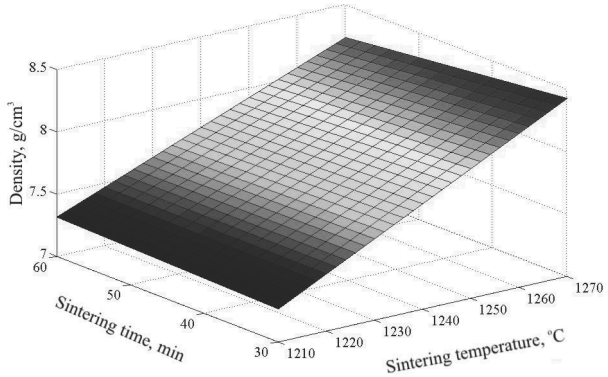

Fig. 5. Regression function plot describing relationship between density and the temperature, and sintering time, for the MG-90HSS/10WC material, sintered in the the vacuum furnace

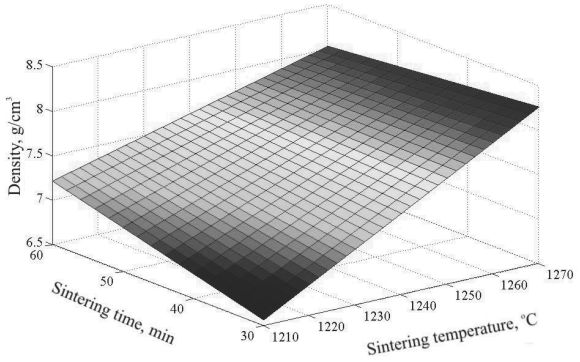

Fig. 8. Regression function plot describing relationship between density and the temperature, and sintering time, for the MG-90HSS/10WC material, sintered in furnace with the atmosphere of the flowing nitrogen with addition of hydrogen (N_2+5%H_2)

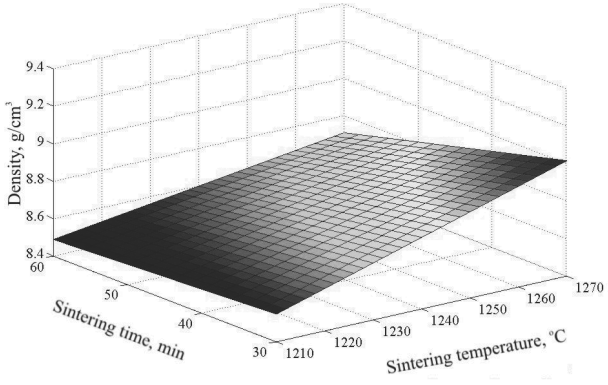

Fig. 6. Regression function plot describing relationship between density and the temperature, and sintering time, for the MG-75HSS/25WC material, sintered in the the vacuum furnace

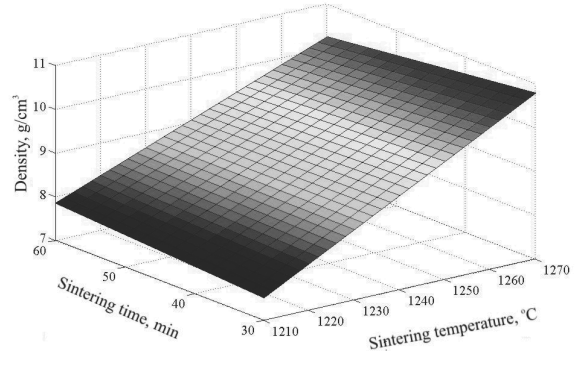

Fig. 9. Regression function plot describing relationship between density and the temperature, and sintering time, for the MG-75HSS/25WC material, sintered in furnace with the atmosphere of the flowing nitrogen with addition of hydrogen (N_2+5%H_2)

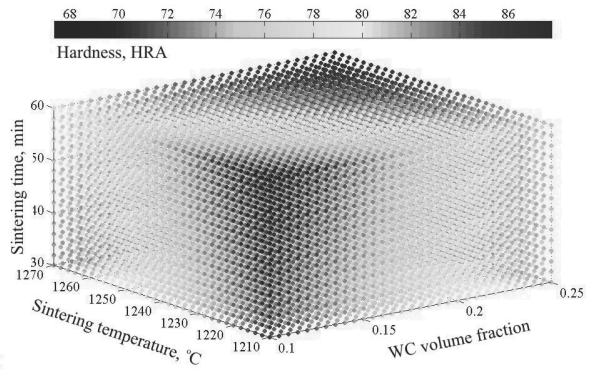

Fig. 10. Regression function plot describing relationship between hardness and the volume fraction of the reinforcing phase, temperature, and sintering time, for the gradient material reinforced with WC carbide, sintered in the vacuum furnace

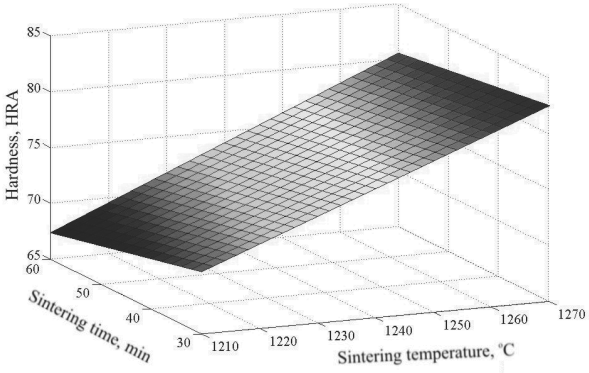

Fig. 11. Regression function plot describing relationship between hardness and the temperature, and sintering time, for the gradient material reinforced with 10% WC carbide, sintered in the vacuum furnace

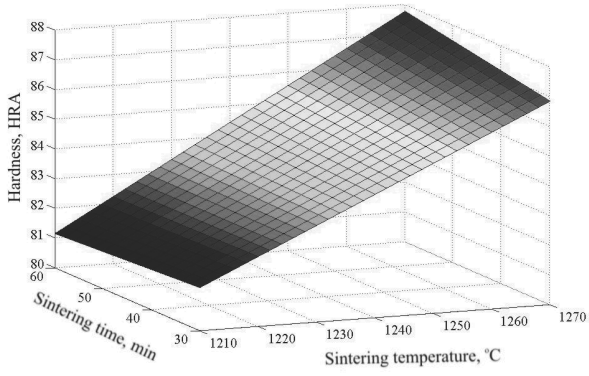

Fig. 12. Regression function plot describing relationship between hardness and the temperature, and sintering time, for the gradient material reinforced with 25% WC carbide, sintered in the vacuum furnace

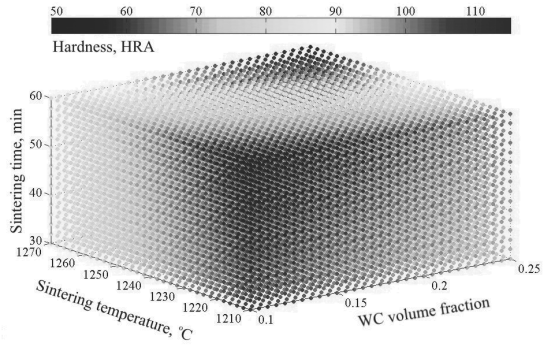

Fig. 13. Regression function plot describing relationship between hardness and the volume fraction of the reinforcing phase, temperature, and sintering time, for the gradient material reinforced with WC carbide, sintered in the furnace with the atmosphere of flowing nitrogen with addition of hydrogen (N_2+5% H_2)

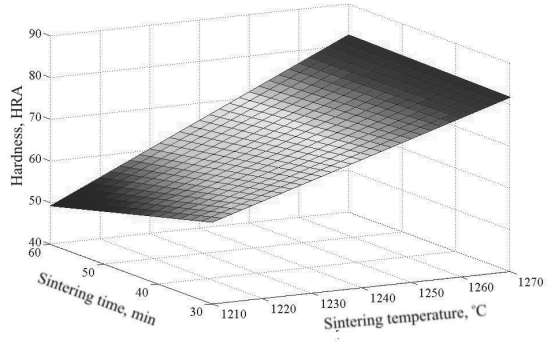

Fig. 14. Regression function plot describing relationship between hardness and the temperature, and sintering time, for the gradient material reinforced with 10% WC carbide, sintered in the furnace with the atmosphere of flowing nitrogen with addition of hydrogen (N_2+5% H_2)

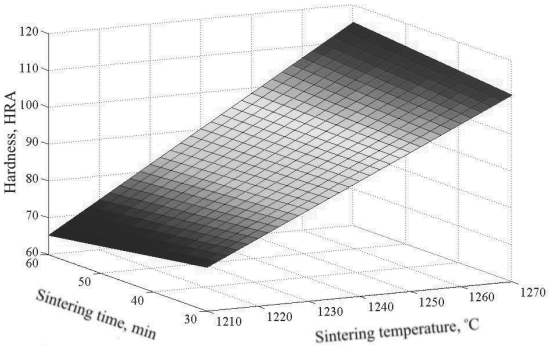

Fig. 15. Regression function plot describing relationship between hardness and the temperature, and sintering time, for the gradient material reinforced with 25% WC carbide, sintered in the furnace with the atmosphere of flowing nitrogen with addition of hydrogen (N_2+5% H_2)

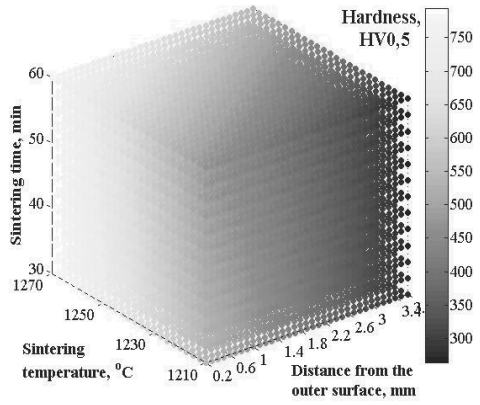

Fig. 16. Regression function plot describing relationship between hardness HV and the distance from the outer surface, temperature, and sintering time, for GM-90HSS/10WC sintered in a vacuum furnace

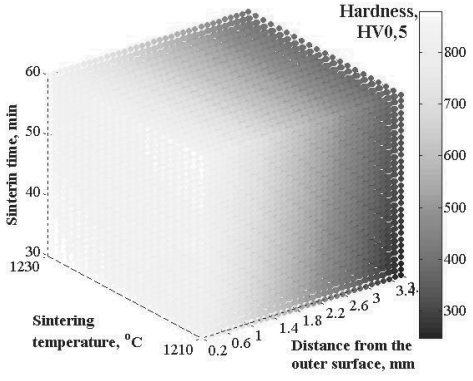

Fig. 17. Regression function plot describing relationship between hardness HV and the distance from the outer surface, temperature, and sintering time, for GM-75HSS/25WC sintered in a vacuum furnace

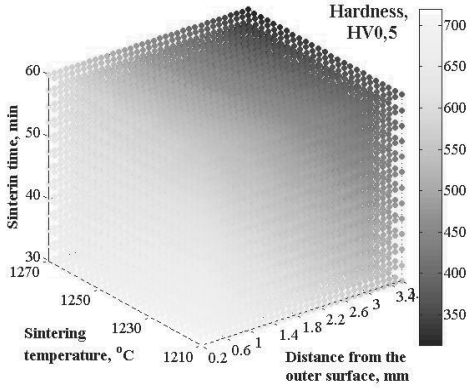

Fig. 18. Regression function plot describing relationship between hardness HV and the distance from the outer surface, temperature, and sintering time, for GM-90HSS/10WC, sintered in the furnace with the atmosphere of the flowing N_2+5% H_2

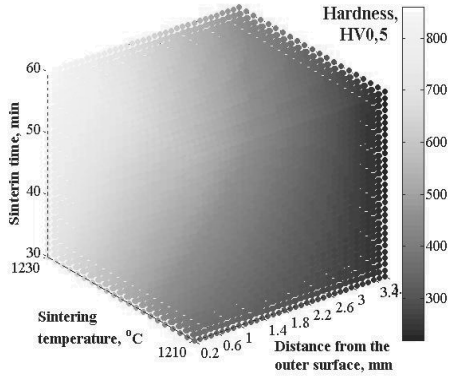

Fig. 19. Regression function plot describing relationship between hardness HV and the distance from the outer surface, temperature, and sintering time, for GM-75HSS/25WC, sintered in the furnace with the atmosphere of the flowing N_2+5% H_2

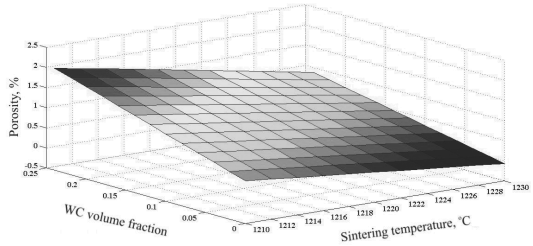

Fig. 20. Regression function plot describing relationship between porosity and the volume fraction of the reinforcing phase and sintering temperature, for the high-speed steel matrix composites reinforced with the WC tungsten carbide, sintered in the vacuum furnace for 30 min

5.2. Structure

The effect of temperature and sintering time on structure of the surface layers containing WC and layers with the high-speed steel alone is shown in Figures 21-24.

Effect of temperature and time is essential in materials containing tungsten carbides. Structure change of the layer with the high-speed steel is discernible for the test piece sintered at the temperature of 1230°C and time of 60 min in test pieces with the 90HSS/10WC surface layer (Figure 21). Some carbides occupy areas with the concave surfaces and have the shape characteristic of the eutectic ones. These areas originated from the liquid state and crystallised as the last ones, among the austenite grains. Temperature increase causes growth and coagulation of the primary carbides. The structure appears characteristic of the remelted high-speed steel. Big carbides are distributed mostly at grain boundaries; whereas, the fine carbides are distributed inside the grains. More and more areas with the eutectic carbides are observed upwards from the temperature of 1250°C and time of 60 minutes. For T_s=1270°C only the elongated narrow carbides are observed distributed at some grain boundaries. The similar structure occurs also in materials with the 75HSS/25WC surface layer (Figure 22).

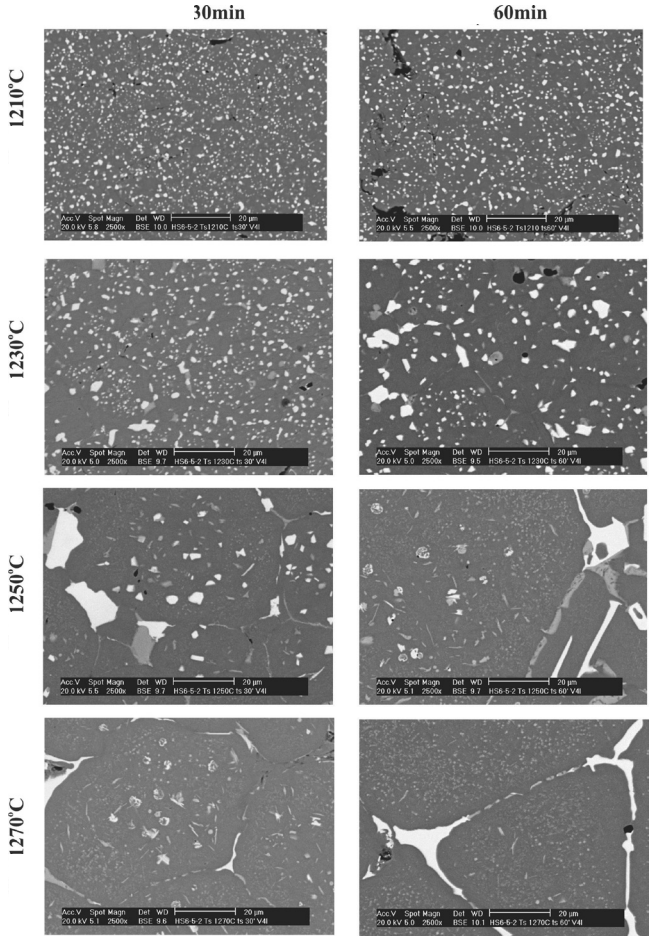

Fig. 21. Structure of the high-speed steel layer of the MG-90HSS/10WC material, sintered in vacuum furnace at temperatures of 1210, 1230, 1250, 1270°C for 30 and 60 min

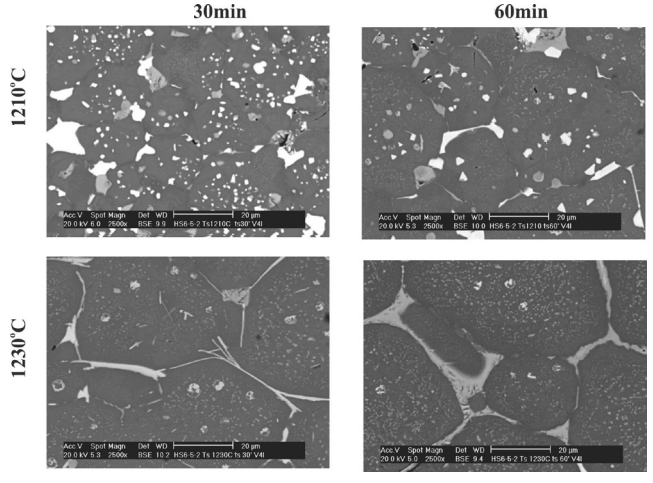

Fig. 22. Structure of the high-speed steel layer of the MG-75HSS/25WC material, sintered in vacuum furnace at temperatures of 1210, 1230, 1250, 1270°C for 30 and 60 min

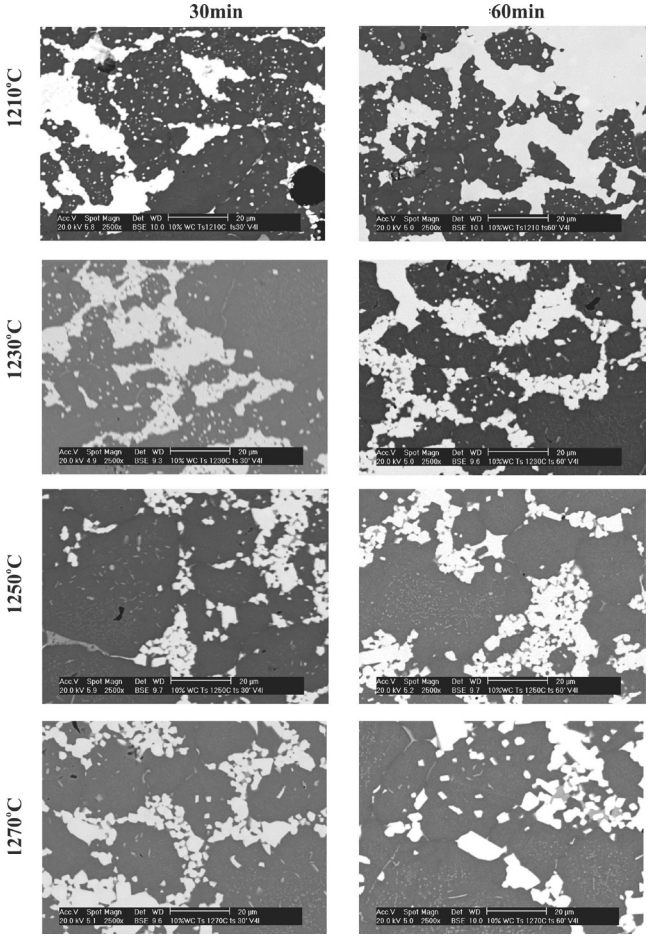

Fig. 23. Structure of the surface layer of the MG-90HSS/10WC material, sintered in vacuum furnace at temperatures of 1210, 1230, 1250, 1270°C for 30 and 60 min

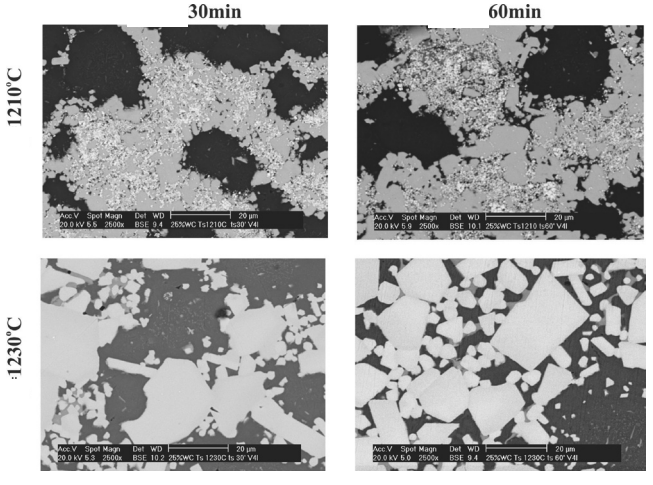

Fig. 24. Structure of the surface layer of the MG-75HSS/25WC material, sintered in vacuum furnace at temperatures of 1210, 1230, 1250, 1270°C for 30 and 60 min

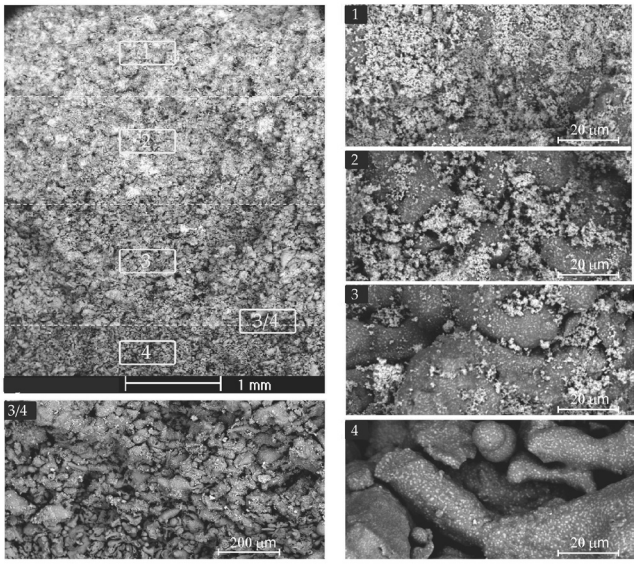

Fig. 25. The green compact photograph as well as its fracture with four layers with the changing WC reinforcing phase portions

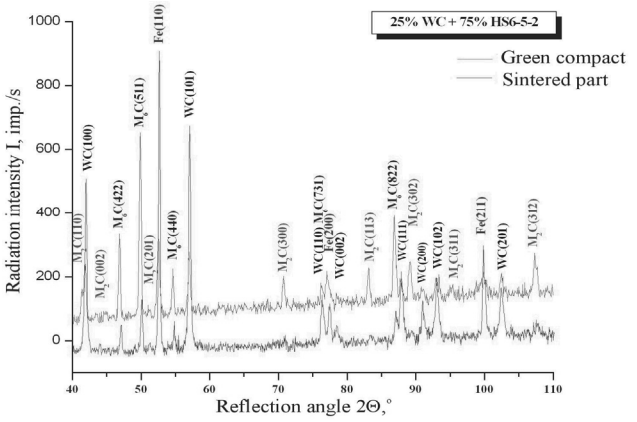

Fig. 26. Results of the X-ray phase analysis for the sintered test piece with the 75HSS/25WC surface layer; diffraction patterns were shifted along the vertical axis to show the results more clearly

Big agglomerations of the tungsten carbides, visible as light areas, occur in the surface layers of materials with the WC tungsten carbide. Eutectic carbides occur only at sintering at the temperature T_s=1250°C and time T_s=30 min (Figure 23). Concentration increase of the tungsten carbides to 25% results in growth of these carbides (Figure 24).

Test piece with the 75HSS/25WC volume composition of the surface layer was selected based on the microstructure observations. The green compact photograph is shown in the Figure 25 as well as its fracture with four layers with the changing WC reinforcing phase portions. The most discernible boundaries are those between the layer from the high-speed steel and the layer with 5% addition of the tungsten carbide. These boundaries vanish along with the WC concentration increase.

It was found out, based on the X-ray diffraction analysis, that the 75HSS/25WC material structure is composed of ferrite, inclusions of tungsten carbide and the MC and M_6C carbides. The new W_2C phase appears in the material due to sintering, the one that does not occur in the structures of the high-speed steel powder or in the sintered high-speed steel (Figure 26) Origination of this phase in the material structure is the effect of the chemical reaction between the high-speed steel and the WC tungsten carbide probably. These results were confirmed during the thin foils examinations (Figure 27).

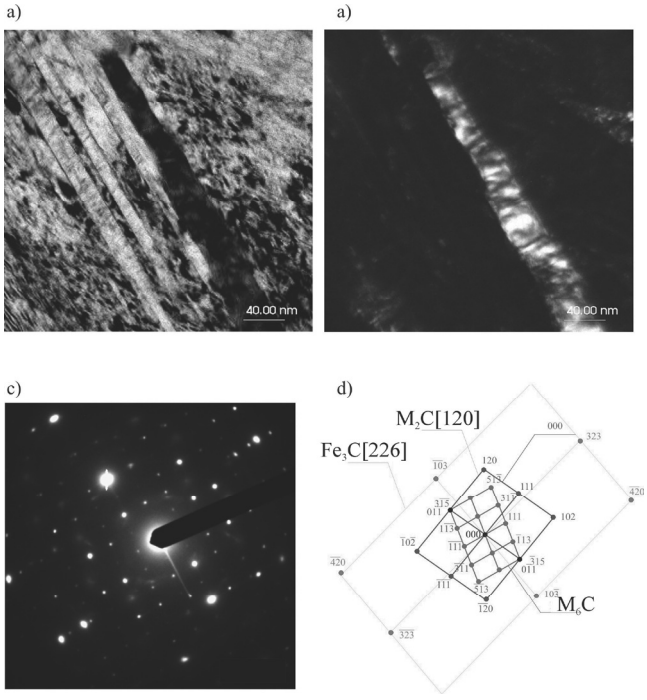

Fig. 27. Structure of thin foil from the surface layer of the MG-75HSS/25WC material, sintered in vacuum furnace at temperature of 1250°C for 60 min; a) image in the bright field, b) image in the dark field, c) diffraction pattern from the area as in Figure a, d) solution of the diffraction pattern from Figure c

5.3. Heat treatment conditions

Regression function plots describing dependence of hardness on austenitizing temperature (T_a), austenitizing time (t_a), and second tempering temperature (T_tII) and their transverse sections in planes specified by the selected input variables values along with the confidence intervals values at the level of α=0.05 are shown in Figures 28-30 for the substrate layers and in Figures 31-33 for the surface layer.

It was shown based on the regression function variability analysis that the effect of heat treatment conditions, in the range assumed in the project, on hardness of the investigated gradient materials in the hardened and tempered state is observable solely in the substrate layers from the high-speed steel only. Hardness tests of the substrate layers of the gradient cermets in the heat treated state demonstrate clear effect of the tempering temperature

on hardness value. The maximum secondary hardness effect of about 66.7 HRC was obtained in the gradient cermets austenitized at the temperature of 1210°C for 80 s, hardened and tempered at the temperature of 560°C. Increasing the tempering temperature to 590°C results in hardness drop compared to the conditions corresponding to the secondary hardness effect by about 1 HRC - in case of materials austenitized at the temperatures of 1180 and 1210°C and by about 2 HRC - for materials austenitized at the temperature of 1150°C. The biggest hardness drop after tempering in the analogous conditions by about 3 HRC was revealed in the substrate layers of the gradient materials previously hardened at the temperature of 1120°C. Hardness of the surface layer of gradient cermets is within the 69.2-71.6 HRC range.

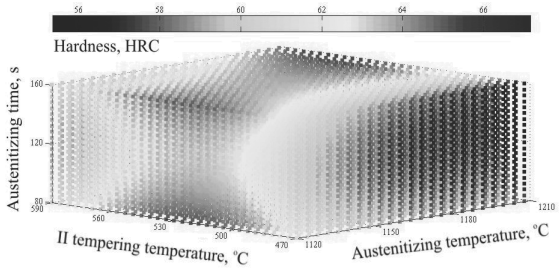

Fig. 28. Regression function plot describing relationship between hardness and the temperature, and austenitizing time, and second tempering temperature for the substrate layer (100% HSS) of the MG-75HSS/25WC

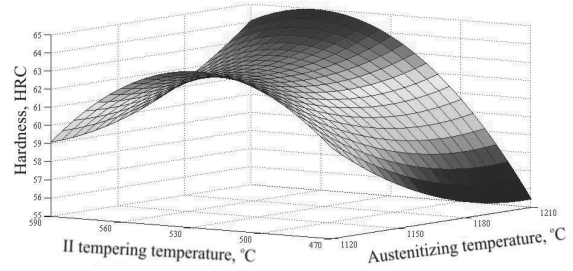

Fig. 29. Regression function plot describing relationship between hardness and the second tempering temperature, and the austenitizing temperature, for the substrate layer (100% HSS) of the MG-75HSS/25WC material austenitized for 120 s

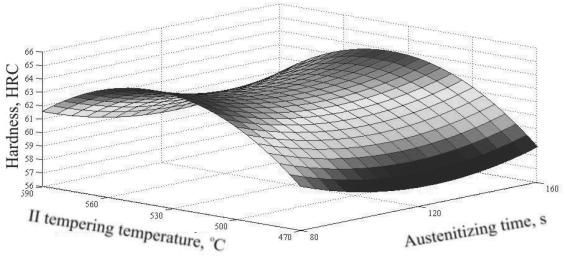

Fig. 30. Regression function plot describing relationship between hardness and the second tempering temperature, and the austenitizing time, for the substrate layer (100% HSS) of the MG-75HSS/25WC material austenitized at the temperature of 1150°C

Carrying out heat treatment in conditions used in the project results in the significant hardness increase in the surface layer of the gradient cermets by 5.8-8.2 HRC up to the values in the 69.2-71.6 HRC range (Figure 31). The highest surface layer hardness of 71.6 HRC is characteristic of the material austenitized at the temperature of 1120°C for 120 s, hardened, and next tempered twice at the temperature of 530°C. No statistically significant effect was found of the heat treatment conditions change in the investigated range on the surface layers hardness after hardening and tempering of the gradient materials containing 25% WC.

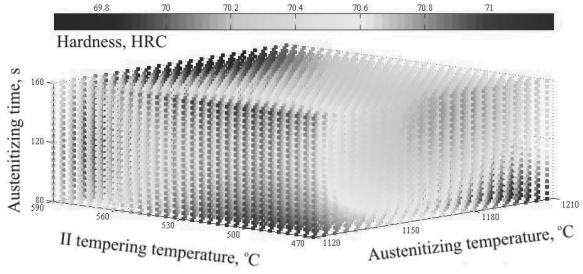

Fig. 31. Regression function plot describing relationship between hardness and the temperature, and austenitizing time, and second tempering temperature for the surface layer (75%HSS+25%WC) of the MG-75HSS/25WC

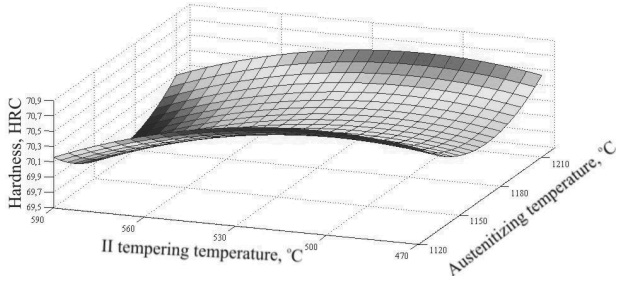

Fig. 32. Regression function plot describing relationship between hardness and the second tempering temperature, and the austenitizing time, for the surface layer (75%HSS+25%WC) of the MG-75HSS/25WC material austenitized for 120 s

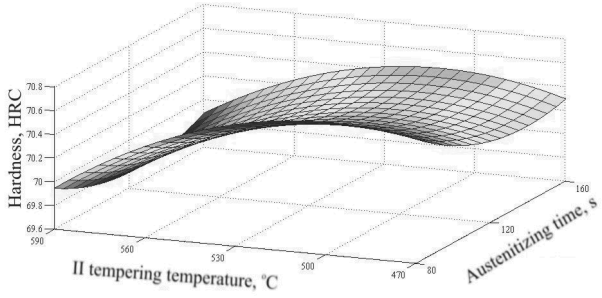

Fig. 33. Regression function plot describing relationship between hardness and the second tempering temperature, and austenitizing time, for the surface layer (75%HSS+25%WC) of the MG-75HSS/25WC material austenitized at the temperature of 1150°C

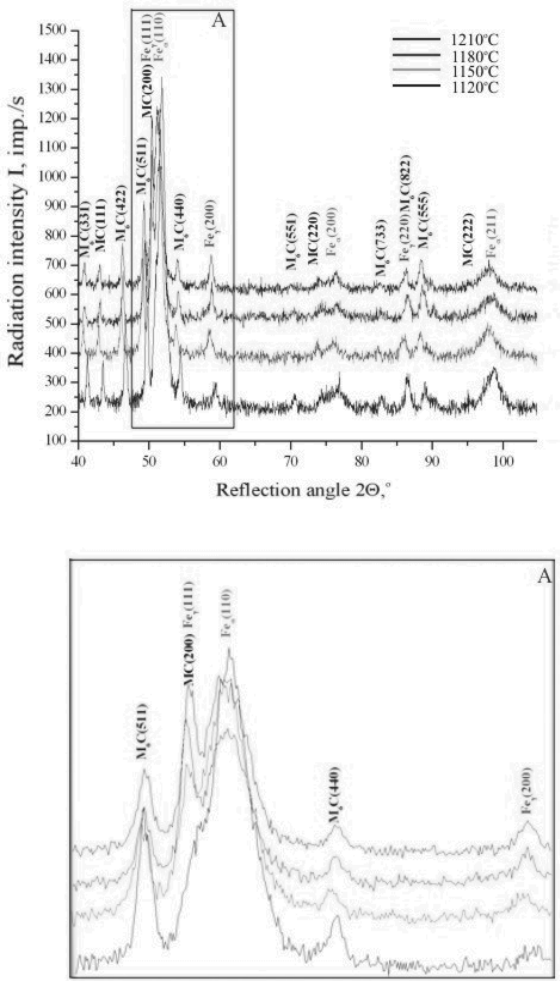

Fig. 34. Results of the X-ray phase analysis from the substrate layer (100% HSS) of the MG-75HSS/25WC test piece, austenitized at temperature of 1210°C for 120 s; diffraction patterns were shifted in respect to the vertical axis to show the results more clearly

Structure of the investigated gradient cermets in the hardened state is martensite with the retained austenite, M_6C and MC type carbides, primary, and also secondary ones, undissolved in the solid solution during austenitizing, as well as the WC tungsten carbides in the surface layer of the materials, which was confirmed with the X-ray phase analysis method (Figure 34). The M_6C and MC type carbides undissolved in the solid solution during austenitizing were idenfied also with the electron diffraction method and observed using the dark field during examinations of the thin foils on the transmission electron microscope (Figure 35).

The primary and secondary carbides, undissolved in the solid solution during austenitizing, affect significantly the primary austenite grain size. Figure 36 present the surface portion analysis results for the carbides, calculated with the quantitative metallography methods. Changes of the primary austenite grain size coefficient according to Snyder-Graff in the substrate layers containing 100% of the HS6-5-2 high-speed steel of the gradient materials, versus temperature and austenitizing time are presented in Figure 37. The substrate layer of the gradient cermet hardened at the temperature of 1120°C and austenitized for 80 s demonstrates the primary grain size of the Snyder-Graff coefficient value of about 12. The primary austenite grain size grows along with the increase of the austenitizing temperature, reaching the Snyder-Graff coefficient value of about 6 after hardening at the temperature of 1210°C. Extending the austenitizing time fosters also growth of the primary austenite grain, whereas, extension of the austenitizing time affects it less than increasing the austenitizing temperature.

The substrate of the investigated gradient cermets in the state hardened at the temperature of 1210°C, which ensures the maximum secondary hardness after tempering, features the martensite with the retained austenite. The volume portion of the retained austenite in the structure of the investigated substrate layers of the hardened gradient cermets depends on the austenitizing conditions. It was found out with the X-ray quantitative phase analysis method that the volume portion of the retained austenite of the hardened test pieces ranges from about 5.7 to 26.5% (Figure 38).

The volume portion of the retained austenite in the substrate layer of the gradient cermets hardened at the temperature of 1210°C, ensuring the maximum secondary hardness after its subsequent tempering at the temperature range from 470 to 590°C gets smaller depending on the second tempering temperature and is within the range from 1.6-23.8% respectively (Figure 39).

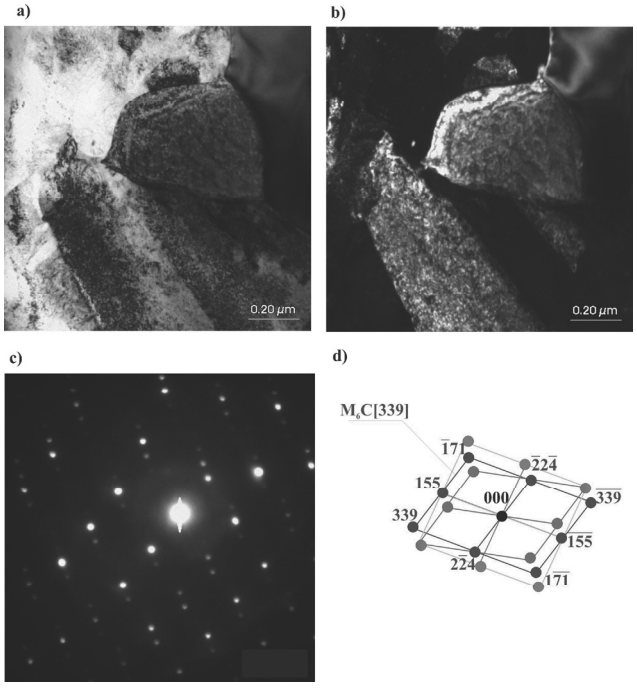

Fig. 35. Structure of thin foil from the surface layer of the MG-75HSS/25WC material, austenitized at temperature of 1150°C for 80 s; a) image in the bright field, b) image in the dark field, c) diffraction pattern from the area as in Figure a, d) solution of the diffraction pattern from Figure c

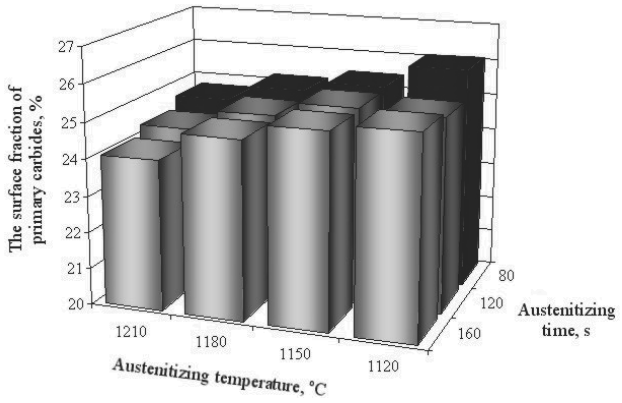

Fig. 36. Relationship between the surface portion of carbides in the substrate layer of the hardened high-speed steel matrix composites, reinforced with the WC carbide phases and austenitizing conditions

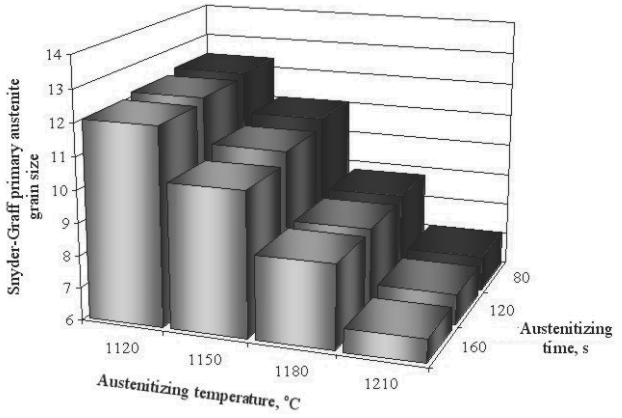

Fig. 37. Relationship between the primary austenite grain size in the substrate layer of the hardened high-speed steel matrix composites, reinforced with the WC carbide phases and austenitizing conditions

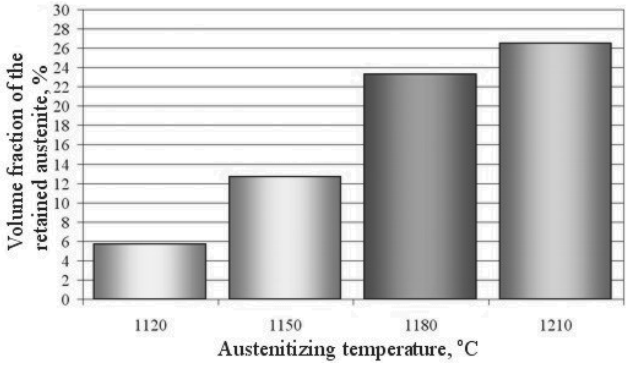

Fig. 38. Relationship between the volume portion of the retained austenite and austenitizing temperature in the substrate layer of the high-speed steel matrix composites, reinforced with the WC carbide phases austenitized for 120 s

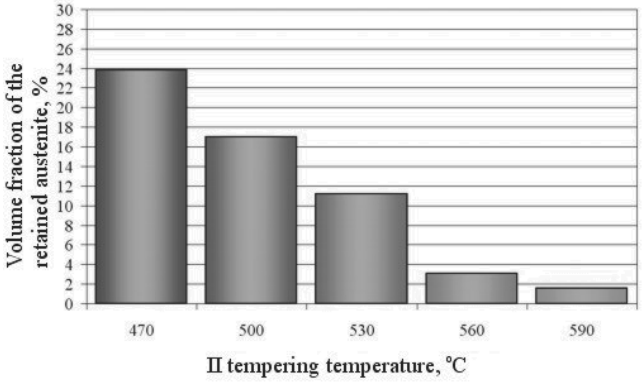

Fig. 39. Relationship between the volume portion of the retained austenite with the second tempering temperature in the substrate layer of the high-speed steel matrix composites, reinforced with the WC carbide phases hardened at temperature of 1210°C after austenitizing for 120 s

The purpose of this study was to prove the effect of carbide in addition to the tribological properties of materials under consideration. Three measurements where performed For each number of cycles. The first profile measurement concerned the layer with the greatest concentration of carbides, and the last steel substrate. The second profile measurement concerned of intermediate layers. It was observed much greater roughness in the region with the greatest concentration of carbides in relation to steel substrate. This phenomena is due to fall out of the carbide less associated with the ground and porous of these layers. Roughness cross-sectional area decreases inversely with the content of the carbides. The wear profiles is shown in Figures 40 and 41. For both numbers of cycles the greater resistance to wear, smaller width and height wear profile was obtained for the layers including highest concentration of carbides Fig. 42.

6. Summary

The conventional powder metallurgy method, consisting in the uniaxial compacting of the powder in a closed die with its subsequent sintering, makes fabrication possible of the gradient cermets with the desired structure and properties by feeding and mixing the substrate powders from the high-speed steel with the hard carbides phases, ensuring the linear change of the reinforcing phases particles portion in the substrate in the direction perpendicular to the surface, while the newly developed materials do not demonstrate cracks and delamination in the boundary zone between the layers, are characteristic of the smooth transition between the layers and demonstrate the linear change of properties.

The MG-75HSS/25WC gradient cermets should be sintered in vacuum, at 1210°C for 30 min at the heating up/cooling rates of 5°C/min to/from the sintering temperature, which ensures material density of about 8.6 g/cm3, surface layer hardness about 81 HRA, porosity about 2%, the substrate layer structure that does not reveal any traces of partial melting.

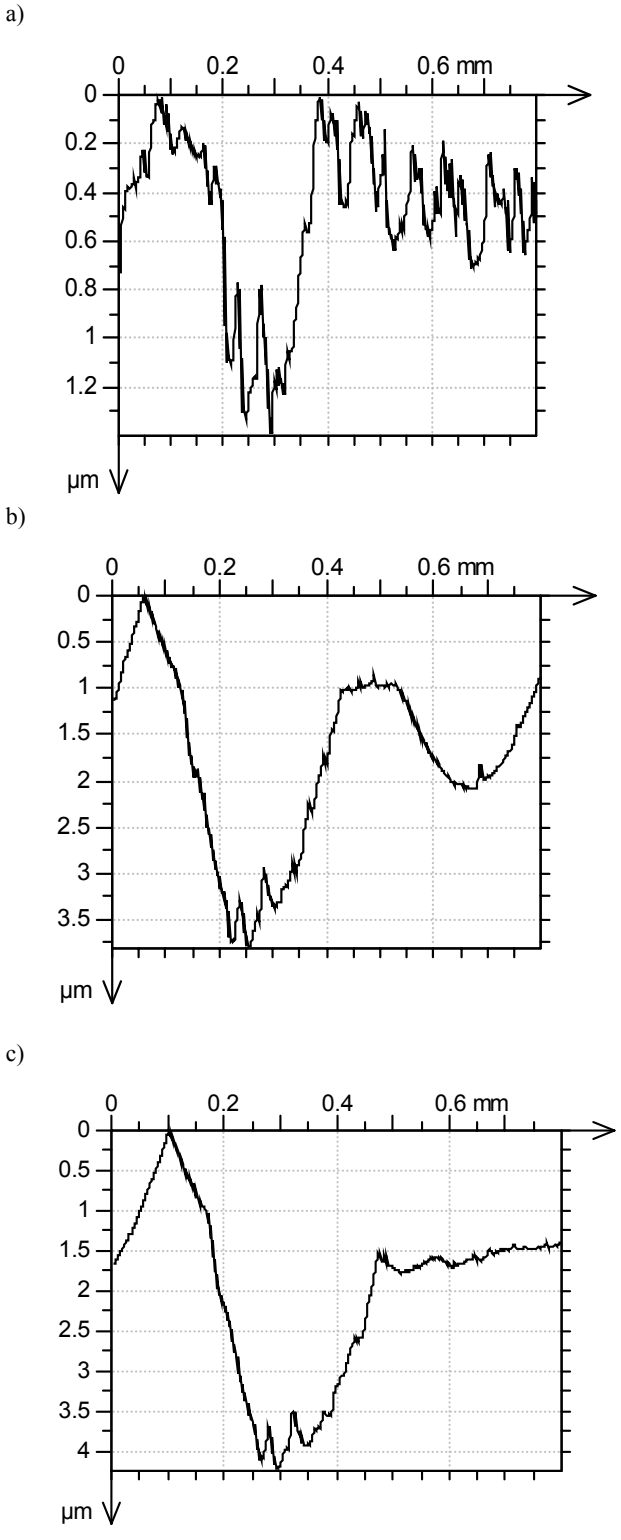

Fig. 40. Wear profile of layers: a) surface rich in the carbides, b) intermediate layers, c) steel substrate - HS6-5-2, after ten thousand cycles; apply load 10 N

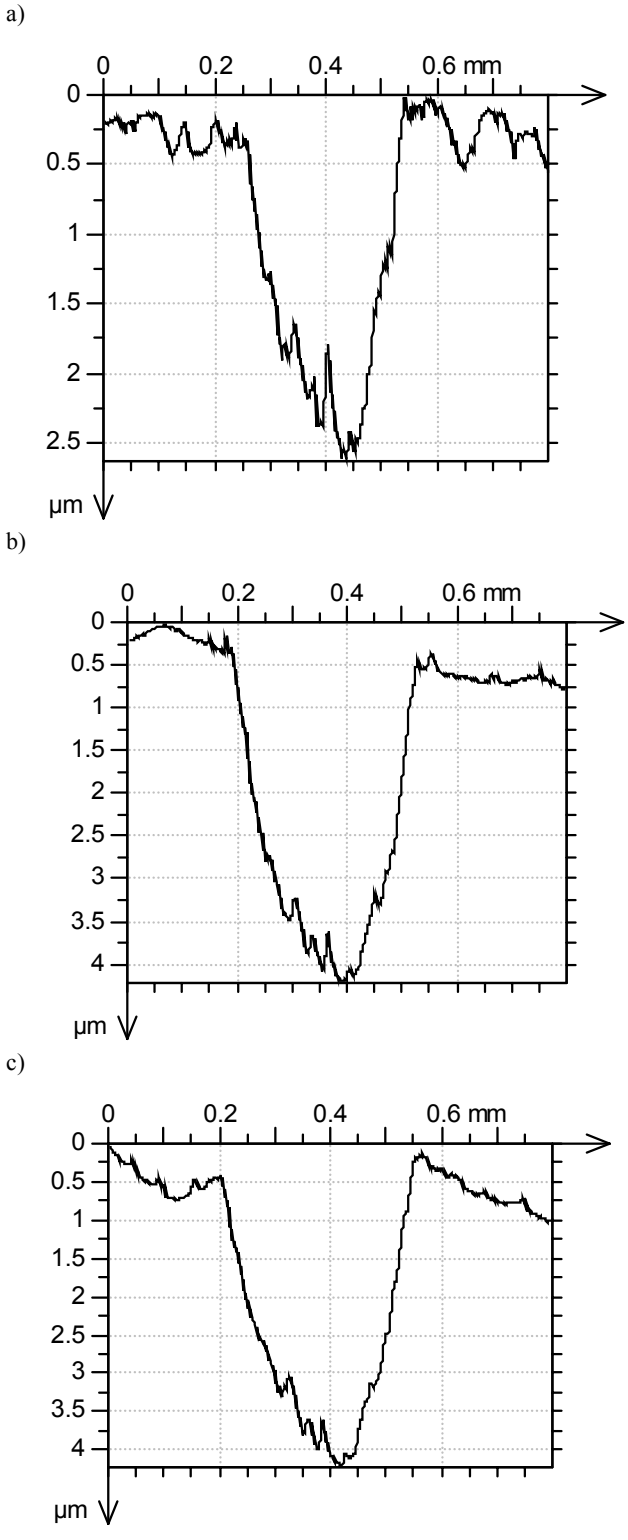

Fig. 41. Wear profile of layers: a) surface rich in the carbides, b) intermediate layers, c) HS6-5-2 steel substrate, after twenty thousand cycles; apply load 10 N

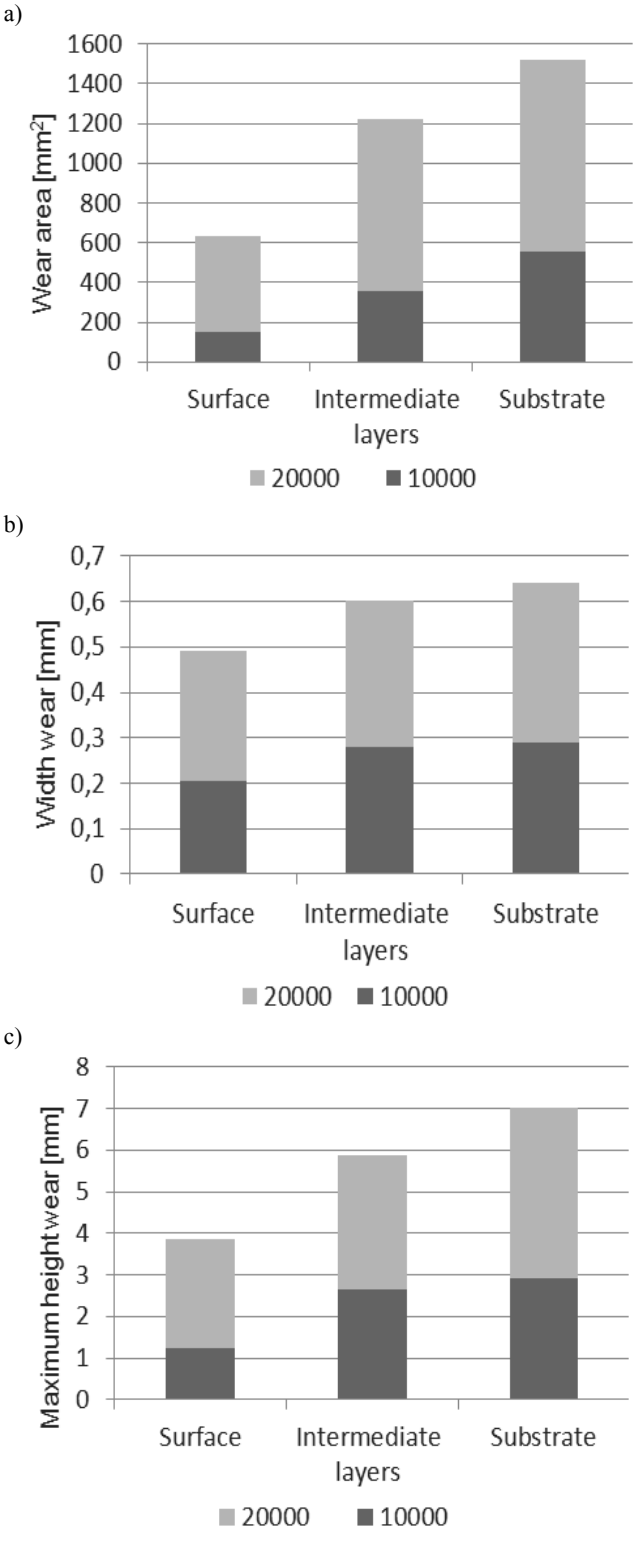

Fig. 42. Relationship between three extreme areas after ten and twenty thousand cycles; a) wear area, b) width wear and c) height wear of the sample; apply load 10 N

Heat treatment of the developed gradient cermets with the core corresponding to the high-speed steel, consisting in hardening and tempering, causes the secondary hardness effect in substrate layers from the high-speed steel by about 2 to 3 HRC higher than hardness of the hardned material. Structure of the MG-75HSS/25WC materials in the hardened state is martensite with the retained austenite, M_6C and MC type carbides, primary, and also secondary ones, undissolved in the solid solution during austenitizing, as well as the WC tungsten carbides in the surface layer. The highest surface layer hardness of 71.6 HRC is characteristic of the material austenitized at the temperature of 1120°C for 120 s, hardened, and next tempered twice at the temperature of 530°C.

The possibility of forming in a wide range of the surface layer hardness of the newly developed gradient cermets reinforced with the WC carbides, depending on their chemical composition and sintering conditions, offers potential for employment of these materials for cutting tools.

It has been proved by the pin on plate test that the addition of the tungsten carbide to the high-speed steel significantly improved the tribological properties.

References

[1] R.F. Bunshah, Handbook of Hard Coatings, William Andrew Publishing/Noyes, 2001.
[2] J.K. Wessel, The Handbook of Advanced Materials: Enabling New Designs, John Wiley and Sons, Incorporated, 2004.
[3] K. Hodor, P. Zięba, B. Olszowska-Sobieraj, Functionally gradient materials as new challenge for modern technology, Materials engineering, XX 6/113 (1999) 595-600 (in Polish).
[4] K. Ichikawa, Functionally graded materials in the 21st century, A workshop on trends and forecasts, Kluwer Academic Publishers, Boston, 2001.
[5] B. Kieback, A. Neubrand, H. Riedel, Processing techniques for functionally graded materials, Materials Science and Engineering A 362 (2003) 81-106.
[6] S. Kirihara, M. Takeda, T. Tsujimoto, Development of Ti/Ti_3Sn functionally gradient material produced by eutectic bonding method, Scripta Materialia 35 (1996) 157-161.
[7] R. Knight, R.W. Smith, Thermal Spray Forming of Materials Powder Metal Technologies and Applications, ASM Handbook, ASM International 7 (1998) 408-419.
[8] A. Maximenko, G. Roebben., O. Van Der Biest, Modelling of metal-binder migration during liquid-phase sintering of graded cemented carbides, Journal of Materials Processing Technology 160 (2005) 361-369.
[9] K. Yamagiwa, Y. Watanabe, K. Matsuda, Y. Fukui, P. Kapranos, Characteristics of a near-net-shape formed $Al-Al_3Fe$ eco-functionally graded material produced over its eutectic melting temperature, Materials Science and Engineering A 416 (2006) 80-91.
[10] H. Yamaoka, Fabrication of functionally gradient materials by slurry stacking and sintering process Ceramic Transactions FGM 34 (1992) 165-172.
[11] Y. Zhang, J. Han, X. Zhang, X. He, Z. Li, S. Du, Rapid prototyping and combustion synthesis of TiC/Ni

functionally gradient materials, Materials Science and Engineering A 299 (2001) 218-224.
[12] L.A. Dobrzański, A. Kloc, G. Matula, Influence of forming on structure and properties of gradient materials, Materials engineering, XXVII 3/151 (2006) 584-587 (in Polish).
[13] L.A. Dobrzański, A. Kloc, G. Matula, J.M. Contreras, J.M. Torralba, Effect of manufacturing methods on structure and properties of the gradient tool materials with the non-alloy matrix reinforced with the HS6-5-2 type high-speed steel, Proceedings of the 11th International Scientific Conference on the Contemporary Achievements in Mechanics, Manufacturing and Materials Science CAM3S'2005, Gliwice-Zakopane, 2005, 223-228.
[14] L.A. Dobrzański, A. Kloc, G. Matula, J. Domagała, J.M. Torralba, Effect of carbon concentration on structure and properties of the gradient tool materials, Journal of Achievements in Materials and Manufacturing Engineering 17 (2006) 45-48.
[15] L.A. Dobrzański, A. Kloc-Ptaszna, G. Matula, J.M. Torralba, Effect of carbon concentration on structure and properties of the gradient tool materials, Founding archives 6/21 (2006) 141-149 (in Polish).
[16] L.A. Dobrzański, A. Kloc-Ptaszna, G. Matula, J.M. Torralba, Structure and properties of the gradient tool materials of unalloyed steel matrix reinforced with HS6-5-2 high-speed steel, Archives of Materials Science and Engineering 28 (2007) 197-202.
[17] L.A. Dobrzański, A. Kloc-Ptaszna, A. Dybowska, G. Matula, E. Gordo, J.M. Torralba, Effect of WC concentration on structure and properties of the gradient tool materials, Journal of Achievements in Materials and Manufacturing Engineering 20 (2007) 91-94.
[18] L.A. Dobrzański, G. Matula, Structure and properties of sintered high speed-steel HS6-5-2 type formed by injection moulding, 3rd Scientific Conference on Materials, Mechanical and Manufacturing Engineering, Gliwice, 2005, 203-210.
[19] L.A. Dobrzański, G. Matula, A. Varez, B. Levenfeld, J.M. Torralba, Structure and Properties of the Heat-Treated High-Speed Steel HS6-5-2 and HS12-1-5-5 Produced by Powder Injection Molding Process, Materials Science Forum 437-438 (2003) 133-136.
[20] L.A. Dobrzański, G. Matula, A. Varez, B. Levenfeld, J.M. Torralba, Fabrication methods and heat treatment conditions effect on tribological properties of high speed steels, Journal of Materials Processing Technology 157 (2004) 324-330.
[21] L.A. Dobrzański, G. Matula, A. Varez, B. Levenfeld, J.M. Torralba, Structure and mechanical properties of HSS HS6-5-2- and HS 12-1-5-5-type steel produced by modified powder injection moulding process, Journal of Materials Processing Technology 157 (2004) 658-668.
[22] L.A. Dobrzański, G. Matula, G. Herranz A. Varez, B. Levenfeld, J.M. Torralba, Influence of debinding process on microstructure and properties of HS6-5-2- HSS parts produced by powder injection molding, 5th International Conference on Industrial Tools ICIT'2005, Cejle, Słowenia, 2005, 189-195.
[23] L.A. Dobrzański, G. Matula, G. Herranz A. Varez, B. Levenfeld, J.M. Torralba, Metal injection moulding of HS12-1-5-5 high-speed steel using a PW-HDPE based binder, Journal of Materials Processing Technology 175 (2006) 173-178.
[24] A. Kloc, L.A. Dobrzański, G. Matula, J.M. Torralba, Effect of manufacturing methods on structure and properties of the gradient tool materials with the non-alloy steel matrix reinforced with the HS6-5-2 type high-speed steel, Materials Science Forum 539-543 (2007) 2749-2754.
[25] G. Matula, L.A. Dobrzański, Structure and properties of TGM manufactured on the basis of HS6-5-2, Journal of Achievements in Materials and Manufacturing Engineering 17 (2006) 101-104.
[26] G. Matula, L.A. Dobrzański, B. Dołżańska, Structure and properties of TGM manufactured on the basis of cobalt, Journal of Achievements in Materials and Manufacturing Engineering 20 (2007) 151-154.
[27] G. Matula, L.A. Dobrzański, G. Herranz, A. Varez, B. Levenfeld, J.M. Torralba, Influence of atmosphere and temperature of debinding on microstructure of HS6-5-2 HSS parts produced by Powder Injection Moulding, Proceedings of the 13th International Conference on "Processing and Fabrication of Advanced Materials" PFAM XIII, Singapur, 2004, 752-761.
[28] G. Matula, L.A. Dobrzański, G. Herranz, A. Varez, B. Levenfeld, J.M. Torralba, Influence of binders on the structure and properties of high speed-steel HS6-5-2 type fabricated using pressureless forming and PIM methods, Materials Science Forum 534-36 (2007) 693-696.
[29] G. Matula, L.A. Dobrzański, G. Herranz, A. Varez, B. Levenfeld, J.M. Torralba, Comparison of structure and properties of HS6-5-2 type high-speed steel fabricated by different powder forming methods, Proceedings of the 11th International Scientific Conference on the "Contemporary Achievements in Mechanics, Manufacturing and Materials Science" CAM3S'2005, Gliwice-Zakopane, 2005, 660-666.
[30] G. Matula, L.A. Dobrzański, M. Mayoral, A. Varez, B. Levenfeld, J.M. Torralba (Eds.), Sintering under different atmospheres of T15 and M2 high speed steels produced by a modified metal injection moulding process, New Developments on Powder Technology, Leganes-Madrid, 2001, 1361-1368.
[31] G. Matula, L.A. Dobrzański, A. Varez, B. Levenfeld, J.M. Torralba (red.), Comparison of structure and properties of the HS12-1-5-5 type high speed steel fabricated using the pressureless forming and PIM methods, Journal of Materials Processing Technology 162 (2005) 230-235.
[32] A. Dobrzańska-Danikiewicz, A. Kloc-Ptaszna, B. Dołżańska, Manufacturing technologies of sintered graded tool materials evaluated according to foresight methodology, Archives of Materials Science and Engineering 50/2 (2011) 69-96.
[33] G. Matula, G. Herranz, A. Varez, B. Levenfeld, J.M. Torralba, L.A. Dobrzański, Microstructure and mechanical properties of T15 high-speed steels parts produced by powder injection moulding using a polyethylene based binder, Proceedings of the Powder Metallurgy World Congers and Exhibition, Vienna, 2004, 469-475.
[34] E. Klar (Eds.), Metals Handbook 7, Powder Metallurgy, American Society for Metals, USA, 1984.
[35] R. Kieffer, W. Hotop, Powder Metallurgy and sintered materials, Publication of PWT, Katowice, 1951 (in Polish).

[36] J. Lis, R. Pampuch, Sintering, Publication of AGH, Cracow, 2000 (in Polish).
[37] J. Nowacki, Metal sintered and the metal matrix composites, Publication of WNT, Warsaw, 2005 (in Polish).
[38] E.M. Ruiz-Navas, E Garcia, E. Gordo, F.J. Velasco, Development and characterisation of high-speed steel matrix composites gradient materials, Journal of Materials Processing Technology 143-144 (2003) 769-775.
[39] L.A. Dobrzański, Principle of materials science, metallography, Publication of WNT, Warsaw, 2006 (in Polish).
[40] L.A. Dobrzański, Metal engineering materials, Publication of WNT, Warsaw, 2004 (in Polish).
[41] M. Wysiecki, Modern tool materials, Publication of WNT, Warsaw, 1997 (in Polish).
[42] L.A. Dobrzański, E. Hajduczek, J. Marciniak, R. Nowosielski, Heat treatment of tool materials, Silesian University of Technology, Gliwice, 1990 (in Polish).
[43] L.A. Dobrzański, E. Hajduczek, J. Marciniak, R. Nowosielski, Metallography and heat treatment of tool materials, Publication of WNT, Warsaw, 1990.
[44] E.M. Ruiz-Navas, E. Gordo, E. Garcia, Development and characterisation of 430L matrix composites gradient materials, Materials Research 8 (2005) 1-4.
[45] W. Włosiński, The joining of advanced materials, Publication of WPW, Warsaw, 1999 (in Polish).
[46] C. Larsson, M. Oden, Hardness profile measurements in functionally graded WC-Co composites, Materials Science and Engineering A 382 (2004) 141-149.
[47] W. Lengauer, K. Dreyer, Functionally graded hardmetals, Journal of Alloys and Compounds 38 (2002) 194-212.
[48] L.A. Dobrzański, A. Kloc, Structure and properties of the gradient tool materials based on a high-speed steel HS-6-5-2 reinforced with WC or VC carbides, Journal of Achievements in Materials and Manufacturing Engineering 37/2 (2009) 213-237.